

Quantitative Evaluation of the Function of Small Intestinal P-Glycoprotein: Comparative Studies Between *in Situ* and *in Vitro*

Yasuhisa Adachi,¹ Hiroshi Suzuki,¹ and
Yuichi Sugiyama^{1,2}

Received February 27, 2003; accepted April 21, 2003

Purpose. The extent of intestinal absorption of MDR1 P-glycoprotein (P-gp) substrate drugs may be affected by interindividual differences in the expression level of P-gp, and/or by simultaneously administered P-gp substrates/inhibitors. The purpose of the present study is to examine whether the extent to which the intestinal absorption is affected by P-gp can be predicted from *in vitro* experiments.

Methods. The *in situ* intestinal perfusion experiments were performed for 12 compounds in *mdr1a/1b* (*-/-*) and normal mice to determine the permeability-surface area (PS) product. Thus determined intestinal P-gp function was compared with the *in vitro* P-gp function, which was determined by comparing the transcellular transport across human P-gp expressing and parental LLC-PK1 monolayers.

Results. *In situ* experimental results revealed that the extent to which the intestinal absorption is affected by P-gp was in the following order; quinidine > ritonavir > loperamide, verapamil, daunomycin > digoxin, cyclosporin A > dexamethasone, and vinblastine. A significant correlation was observed between P-gp function determined in the intestinal perfusion and that in LLC-PK1 monolayers.

Conclusion. The *in vitro* transcellular transport across P-gp expressing monolayers may be used to predict the extent to which the intestinal absorption is affected by P-gp.

KEY WORDS: MDR1 P-glycoprotein; intestinal absorption; intestinal perfusion; jejunum; *mdr1* knockout mice, LLC-PK1.

INTRODUCTION

MDR1 P-glycoprotein (P-gp) was initially cloned from the multidrug-resistant tumor cell lines as an ATP-dependent transporter responsible for the cellular extrusion of a series of antitumor drugs (1,2). It is now well established that P-gp is also expressed in many normal tissues, including the intestinal epithelium, hepatocytes, renal tubular cells, and brain capillary endothelial cells, and plays an important role in drug disposition (3–5). The contribution of P-gp to the disposition of many drugs has been investigated by using *mdr1* knockout mice for many years (6).

In particular, the contribution of P-gp in lowering the oral bioavailability has been demonstrated by comparing the disposition of orally administered substrate drugs, such as taxol (7,8), digoxin (9), tacrolimus (10), and saquinavir (11,12) between normal and *mdr1a* (*-/-*) and/or *mdr1a/1b* (*-/-*) mice. In addition, several reports suggest that P-gp also has an important role in lowering the intestinal absorption in

humans. These include the findings 1) that the oral bioavailability of digoxin and cyclosporin A correlates well with the amount of P-gp expressed in the small intestine (13,14); 2) that the intake of grapefruit juice containing substrates that inhibit the P-gp function results in the increased oral bioavailability of cyclosporin A (15); and 3) that the induction of intestinal P-gp results in the reduced bioavailability of digoxin (13). In addition, although the results are still controversial (16), several reports indicate that the plasma area under the curve of substrate drugs is higher in subjects whose intestinal P-gp expression is lower due to the polymorphism in exon 26 (C3435T; Refs. 17–19).

Taking these results into consideration, it is possible that the variation in the intestinal absorption of substrate drugs due to interindividual differences in the expression level of intestinal P-gp and that due to simultaneously administered P-gp substrates/inhibitors may depend on the extent to which the intestinal absorption of each drug is affected by P-gp. In the present study, we determined the quantitative role of P-gp in lowering the oral absorption of its substrates, and also examined whether intestinal P-gp function could be predicted from *in vitro* experiments. Because we and others have previously reported that the P-gp function in the blood–brain barrier (BBB) correlates well with the transcellular transport across the human P-gp expressing LLC-PK1 monolayer (20,21), we also examined the correlation of P-gp function between the small intestine and the BBB.

MATERIAL AND METHODS

Chemicals

[³H]Daunomycin (185 GBq/mmol), [³H]digoxin (703 GBq/mmol), [³H]diazepam (3052 GBq/mmol), [³H]dexamethasone (1500 GBq/mmol), [³H]progesterone (5291 GBq/mmol), [³H]verapamil (3145 GBq/mmol), and [¹⁴C]inulin (1.85 GBq/mmol) were purchased from New England Nuclear (Boston, MA, USA). [³H]Cimetidine (574 GBq/mmol), [³H]cyclosporin A (259 GBq/mmol), and [³H]vinblastine (412 GBq/mmol) were obtained from Amersham (Buckinghamshire, UK). [³H]Quinidine (740 GBq/mmol) was a product of ARC (St. Louis, MO, USA). [³H]Ritonavir (37 GBq/mmol) was purchased from Moravек (Brea, CA, USA). [³H]Loperamide (185 GBq/mmol), synthesized by tritium gas exchange methods, was purchased from TRITEC AG (Teufen, Switzerland). PSC833 was kindly gifted from Novartis (Basel, Switzerland). All other unlabeled compounds were purchased from Sigma (St. Louis, MO, USA).

Animals

Experiments were performed in *mdr1a/1b* (*-/-*) mice (Taconic Farms Inc., NY, USA). FVB mice (Taconic Farms Inc., NY, USA) were used as the control mice. All mice were housed individually in a cage with paper bedding (alpha-dry, Shepherd Specialty Papers, Kalamazoo, MI, USA) at controlled conditions (23°C, 55% air humidity, 12-h light cycle). The mice were acclimatized for at least 1 week before the experiments and had access to tap water and rodent pellet food (MF, Oriental Yeast Co. Ltd., Tokyo).

¹ School of Pharmaceutical Sciences, The University of Tokyo, Hongo, Bunkyo-ku, Tokyo 113-0033, Japan.

² To whom correspondence should be addressed. (e-mail: sugiyama@mol.f.u-tokyo.ac.jp)

Jejunum Perfusion Experiments

The perfusion experiments were performed according to the methods described previously (22–24). Mice weighing 27–32 g were fasted overnight before the perfusion experiment with access to tap water only. Anesthesia was induced with an intravenous injection of Nembutal® (Dainippon Pharmaceuticals, Osaka, Japan) (pentobarbital sodium, 50 mg/kg), and the mice were placed on a heating pad to maintain a body temperature at 37°C. The abdomen was opened by a midline longitudinal incision and a 8–10 cm jejunal segment was isolated and cannulated at both ends with plastic tubing. The segment was rinsed with phosphate-buffered saline (pH 6.4). Saline was dropped onto the surgical area, which was then covered with a paper sheet to avoid loss of fluid. The experiment was initiated by filling the segment with a 1-mL bolus of the perfusion solution followed by perfusion at 0.1 mL/min using an infusion pump (Harvard Apparatus Syringe Infusion Pump, South Natick, MA, USA). The perfusion solution consisted of 20.1 mM Na₂HPO₄, 47.0 mM KH₂PO₄, 101 mM NaCl (pH 6.4), and contained tritium-labeled probes with a tracer concentration of ¹⁴C-labeled inulin as a nonabsorbable marker (23). The concentrations of the probes were as follows: [³H]daunomycin (9.25 KBq/mL, 50 nM), [³H]digoxin (9.25 KBq/mL, 13 nM), [³H]diazepam (9.25 KBq/mL, 3 nM), [³H]dexamethasone (9.25 KBq/mL, 6 nM), [³H]progesterone (9.25 KBq/mL, 1.5 nM), [³H]verapamil (9.25 KBq/mL, 3 nM), [³H]cimetidine (9.25 KBq/mL, 16 nM), [³H]cyclosporin A (9.25 KBq/mL, 9 nM), [³H]vinblastine (9.25 KBq/mL, 6 nM), [³H]quinidine (9.25 KBq/mL, 13 nM), [³H]ritonavir (9.25 KBq/mL, 250 nM), and [³H]loperamide (9.25 KBq/mL, 50 nM). The outflow perfusate was collected at 5-min intervals for 60 min. The length of the segment was measured at the end of experiments. Scintillation cocktail (Hionic-fluor, Packard, Meriden, CT, USA) was added to the aliquots removed from the samples and their radioactivities were measured in a liquid scintillation counter (model 2700 TR, Packard, Meriden, CT, USA).

Data Analysis

The absorbed fraction (F_a) of each ligand was estimated according to the following equation, which corrects for the volume change using [¹⁴C]inulin as a nonabsorbable marker (23):

$$F_a = 1 - \frac{C_{in,I}}{C_{out,I}} \times \frac{C_{out}}{C_{in}} \quad (1)$$

where $C_{in,I}$ and $C_{out,I}$ represent the concentration of [¹⁴C]inulin in the inflow and outflow solutions, respectively, and C_{in} and C_{out} represent the ligand concentration in the inflow and outflow solutions, respectively.

The apparent membrane permeability clearance, or the product of the apparent membrane permeability coefficient and the surface area, for the unit length of intestinal segments was calculated as follows (23);

$$\text{PS product} = -\frac{Q}{L} \times \ln(1 - F_a) \quad (2)$$

where PS product is the product of the apparent membrane permeability coefficient and the surface area, Q is the perfu-

sion rate (0.1 mL/min), and L is the length of perfused segments.

RESULTS

The PS product of 12 compounds was determined in normal and *mdr1a/1b* (–/–) mice using the *in situ* intestinal perfusion technique. The time profiles for the F_a of ligands are shown in Fig. 1. It was revealed that the F_a of typical P-gp substrates such as quinidine and verapamil in *mdr1a/1b* (–/–) mice was significantly higher than those in normal mice, whereas no significant difference was observed in poor substrates for P-gp (such as diazepam) between the two strains (Fig. 1). The mean values of the F_a between 20 and 30 min were used to determine the PS product for these ligands. Although much longer time was required to reach the steady state conditions for some compounds including cyclosporin A and daunomycin, we calculated the PS product for such compounds by using the F_a obtained between 20 and 30 min, due to the difficulties in maintaining the viability of mice for much longer time.

To further support the propriety of the experimental conditions, we examined the effect of PSC833, an inhibitor for P-gp, on the intestinal absorption of [³H]quinidine. As shown in Fig. 2, PSC 833 (1 μM) significantly increased the absorption of [³H]quinidine in normal mice, but not in *mdr1a/1b* (–/–) mice. In contrast, PSC 833 (1 μM) did not significantly affect the absorption of [³H]quinidine in *mdr1a/1b* (–/–) mice (Fig. 2), suggesting that the intestinal P-gp function can be determined from these experimental conditions.

In addition, the amount of ligands remaining in the intestinal mucosa was also determined in normal and *mdr1a/1b* (–/–) mice at the end of experiments. It was revealed that the intestinal content of typical P-gp substrates such as quinidine, loperamide and vinblastine was significantly higher in *mdr1a/1b* (–/–) mice than normal mice (Fig. 3), which is consistent with the fact that P-gp is located on the apical membrane and, therefore, reduce the intestinal absorption of its substrates.

To evaluate the function of P-gp quantitatively, the intestinal PS product ratio was determined by dividing the PS products in *mdr1a/1b* (–/–) mice by those in normal mice. As shown in Table I, the PS product ratio was in the order, quinidine > ritonavir > loperamide, verapamil, daunomycin > digoxin, cyclosporin A > dexamethasone and vinblastine. These ratios were also compared with those determined *in vitro*. Previously, we have determined the transcellular transport of 12 ligands across human P-gp-expressing and parental LLC-PK1 monolayer (20). In the present study, we calculated the *in vitro* PS product ratio (PS_{a-to-b} ratio) by dividing the PS product for the apical-to-basal flux across parental LLC-PK1 monolayer by that across P-gp-expressing monolayer. These values are summarized in Table II. A significant correlation in the PS product ratios between *in situ* and *in vitro* was obtained (Fig. 4).

Finally, we compared the function of P-gp between the small intestine and the BBB. For the P-gp function in the BBB, we have cited the previously reported $K_{p, \text{brain}}$ ratios, which were defined as the brain-to-plasma concentration ratio in *mdr1a/1b* (–/–) mice divided by the same ratio in normal mice (20). Although the correlation was significant for 12 compounds, the plot for some compounds such as digoxin was not superimposable on the correlation line (Fig. 5).

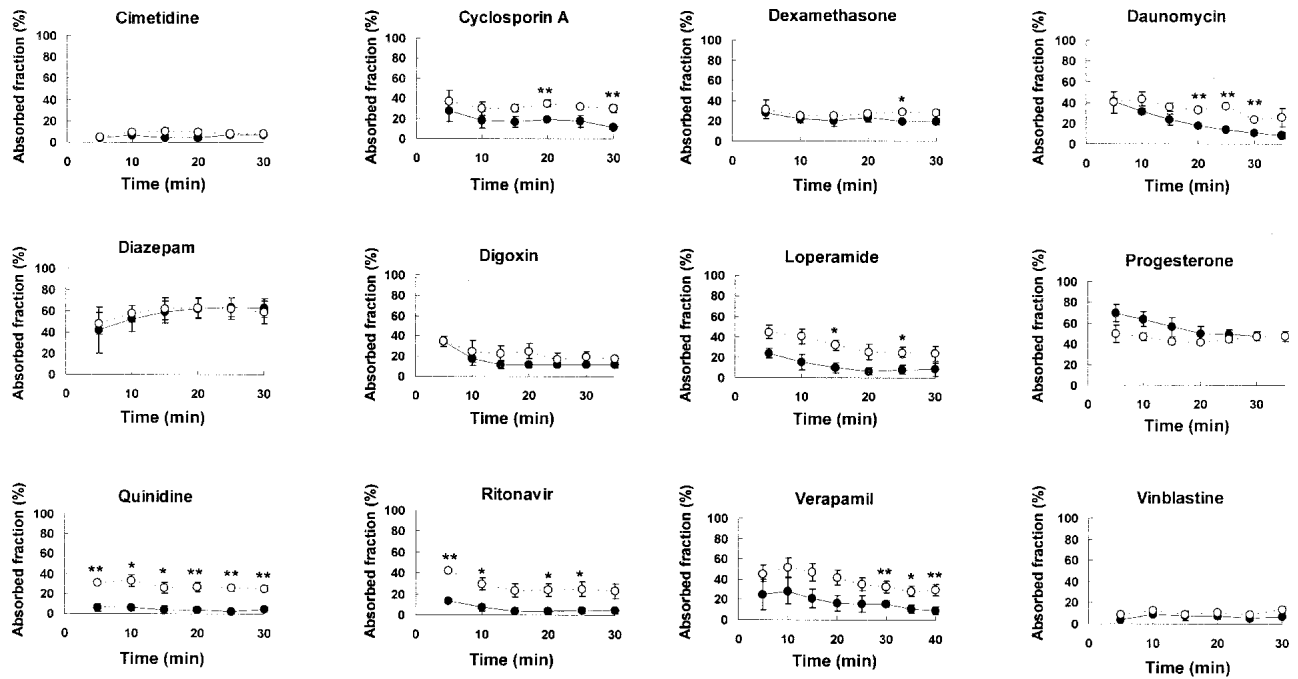


Fig. 1. Time profiles for the absorbed fraction of ligands in the outflow. The small intestinal segments were perfused with the medium containing isotopically labeled compounds to determine the outflow concentrations. The results are given as the absorbed fraction, defined by Eq. (1) in the text. Each point and vertical bar represents the mean \pm SE of three independent determinations. Open and closed circles represent the results in *mdr1a/1b(-/-)* and normal mice respectively. Statistical difference in *mdr1a/1b(-/-)* mice were compared to normal mice by two-sided Student's *t* test with $p < 0.05$ as the limit of significance (* $p < 0.05$; ** $p < 0.01$).

DISCUSSION

In the present study, we have quantitatively determined the contribution of P-gp in lowering the oral bioavailability by using an *in situ* intestinal perfusion technique in normal and *mdr1a/1b(-/-)* mice. For substrates that are extensively transported by P-gp, there was a significant difference in the absorbed fraction between normal and *mdr1a/1b(-/-)* mice

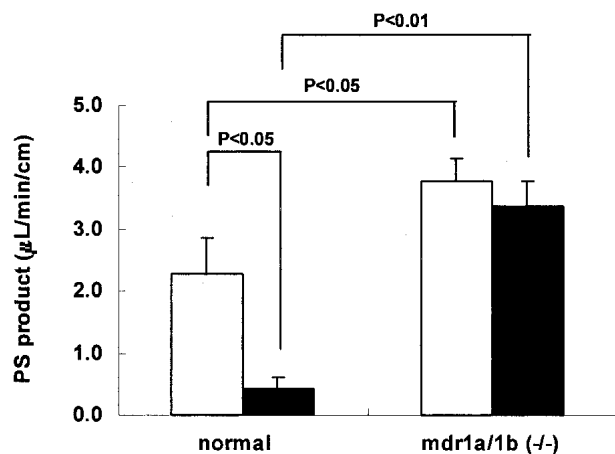


Fig. 2. Effect of PSC833 on the intestinal absorption of [3 H]quinidine. The PS product for [3 H]quinidine in normal and *mdr1a/1b(-/-)* mice was determined in the presence and absence of PSC833 (1 μ M). Each point and vertical bar represents the mean \pm SE of three independent experiments. Open and closed bars represent the results in the presence and absence of PSC 833, respectively. Statistical differences were compared by two-sided Student's *t* test with $p < 0.05$ as the limit of significance.

(Fig. 1), and in addition, the amount remaining in the intestinal mucosa at the end of experiments was much higher in *mdr1a/1b(-/-)* mice than in normal mice (Fig. 3). In order to evaluate the contribution of P-gp to decreasing the intestinal absorption, we have determined the *in situ* intestinal PS product ratio. As shown in Table I, the intestinal PS product ratio was in the order, quinidine > ritonavir > loperamide, verapamil, daunomycin > digoxin, cyclosporin A > dexamethasone and vinblastine. These values may be compared to the previously reported oral absorption of the ligands in normal and *mdr1a/1b(-/-)* mice. The intestinal PS product ratio for digoxin was 2.06 ± 0.07 (Table I), which is similar to the ratio of plasma concentrations in *mdr1a/1b(-/-)* mice after oral administration to that in normal mice (1.7; Ref. 9). Moreover, in human subjects who have homozygous T allele at position 3435, the intestinal P-gp level was approximately one tenth that of homozygous C/C genotype, and consequently, the plasma AUC of digoxin after oral administration was approximately two times higher than that of wild type subjects (17). This value is also consistent with the intestinal PS product ratio of digoxin determined in the present study (Table I). These results may have some clinical implications. The intestinal absorption of P-gp substrate drugs with high PS product ratios may be markedly affected by interindividual differences in the expression level of P-gp and/or by simultaneously administered P-gp substrates/inhibitors, whereas those with low PS product ratios may only be minimally affected by an alteration in P-gp function.

We also found a significant correlation in the PS product ratio between *in situ* and *in vitro* experiments. The *in situ* and *in vitro* PS product ratios will be discussed by considering a pharmacokinetic model for the transcellular transport

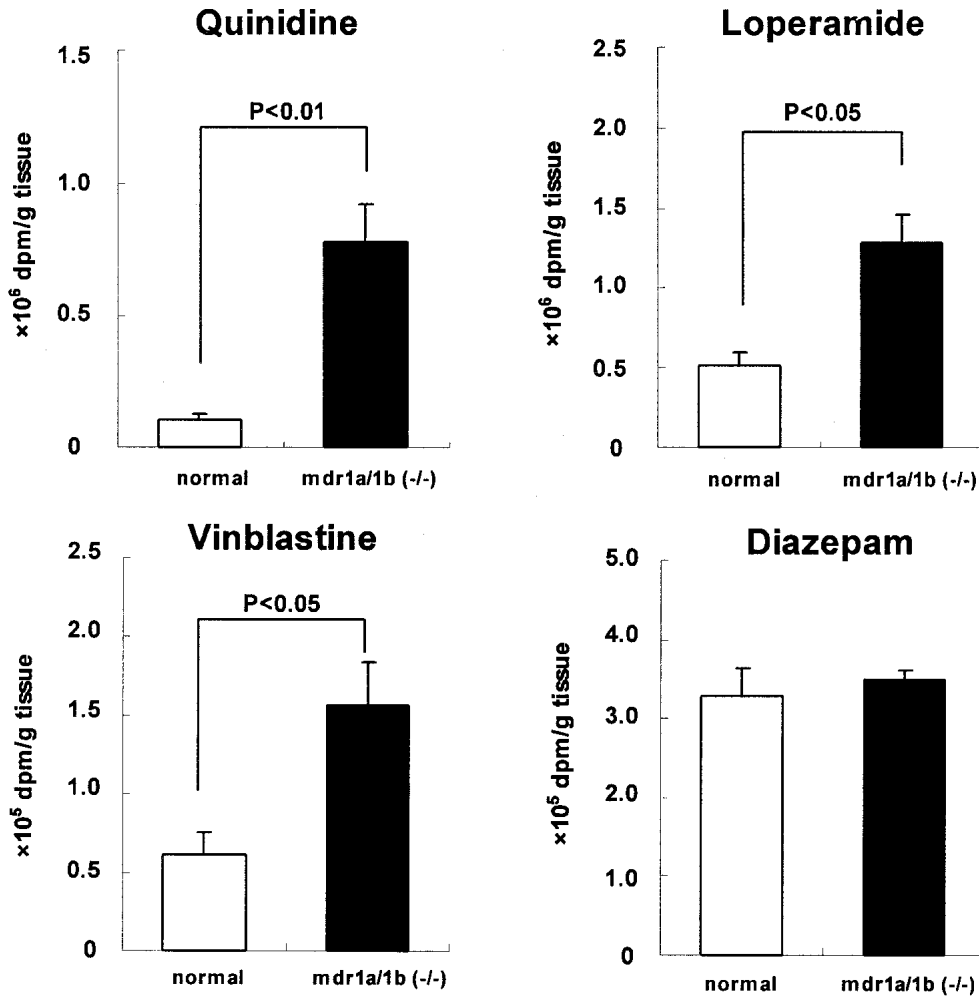


Fig. 3. Content of ligands remaining in the intestine. Content of ligands remaining in the intestine of normal and *mdr1a/1b* (*-/-*) mice was determined at the end of experiments. Each point and vertical bar represents the mean \pm SE of three independent experiments. Open and closed bars represent the results in normal and *mdr1a/1b* (*-/-*) mice respectively. Statistical difference in *mdr1a/1b* (*-/-*) mice were compared to normal mice by two-sided Student's *t* test with $p < 0.05$ as the limit of significance.

(Scheme 1). The PS products for the intestinal absorption in normal and *mdr1a/1b* (*-/-*) mice are given by the following equations:

PS product in normal mice =

$$PS_{m,inf} \times \frac{PS_{s,eff}}{PS_{m,eff} + PS_{s,eff} + PS_{P-gp}} \quad (3)$$

PS product in *mdr1a/1b* (*-/-*) mice =

$$PS_{m,inf} \times \frac{PS_{s,eff}}{PS_{m,eff} + PS_{s,eff}} \quad (4)$$

where $PS_{m,inf}$ and $PS_{m,eff}$ represent the PS product for the influx and efflux across the mucosal membrane respectively, and $PS_{s,eff}$ represents the PS product for the efflux across the serosal membrane of the intestinal epithelial cells (Scheme 1). Consequently, the intestinal PS product ratio is calculated by dividing the PS product in *mdr1a/1b* (*-/-*) mice by that in normal mice:

$$PS \text{ product ratio} = 1 + \frac{PS_{P-gp}}{PS_{m,eff} + PS_{s,eff}} \quad (5)$$

In the same manner, the PS product for the transcellular transport (apical-to-basal flux) across the parental and P-gp expressing LLC-PK1 monolayers is given by the following:

PS_{a-to-b} in MDR1 expressing cells =

$$PS_{a,inf} \times \frac{PS_{b,eff}}{PS_{a,eff} + PS_{b,eff} + PS_{P-gp}} \quad (6)$$

$$PS_{a-to-b} \text{ in parental cells} = PS_{a,inf} \times \frac{PS_{b,eff}}{PS_{a,eff} + PS_{b,eff}} \quad (7)$$

Then, the PS_{a-to-b} ratio is given by the following:

$$PS_{a-to-b} \text{ ratio} = 1 + \frac{PS_{P-gp}}{PS_{a,eff} + PS_{b,eff}} \quad (8)$$

Comparison of Eqs. (5) and (8) provides the theoretical basis for the presence of a significant correlation in the PS product ratio between *in situ* and *in vitro* is observed (Fig. 4).

However, the correlation in the P-gp function between *in vitro* and *in situ* intestinal absorption (Fig. 4) was less than that obtained between *in vitro* and *in vivo* BBB penetration (20). We have previously observed that the function of P-gp in

Table I. PS Products Determined in the *in Situ* Intestinal Perfusion

Drugs	PS product ($\mu\text{L}/\text{min}/\text{cm}$)		PS product ratio
	Normal	mdr1a/1b(-/-)	
Cimetidine	0.973 \pm 0.089	0.928 \pm 0.075	0.95 \pm 0.13
Cyclosporin A	2.13 \pm 0.21	4.27 \pm 0.32**	2.01 \pm 0.24
Daunomycin	1.63 \pm 0.20	4.91 \pm 0.29**	3.01 \pm 0.40
Dexamethasone	2.38 \pm 0.23	3.92 \pm 0.45*	1.65 \pm 0.09
Diazepam	13.0 \pm 2.8	12.8 \pm 3.4	0.99 \pm 0.34
Digoxin	1.14 \pm 0.15	2.34 \pm 0.12*	2.06 \pm 0.07
Loperamide	1.10 \pm 0.77	3.44 \pm 0.90	3.14 \pm 2.35
Progesterone	8.23 \pm 0.96	7.63 \pm 0.88	0.93 \pm 0.15
Quinidine	0.428 \pm 0.190	3.36 \pm 0.41**	7.86 \pm 3.63
Ritonavir	0.564 \pm 0.314	2.64 \pm 0.79	4.70 \pm 2.98
Verapamil	1.38 \pm 0.51	4.23 \pm 0.13**	3.07 \pm 1.14
Vinblastine	0.926 \pm 0.106	1.25 \pm 0.11	1.35 \pm 0.20

Note: The PS products for the intestinal absorption were calculated from the data shown in Fig. 1 using Eq. (2). The values of *in situ* PS product ratio, defined as the PS product in mdr1a/1b (-/-) mice divided by the same value in normal mice, were also calculated. The results are shown as the mean \pm SE. The SE for the PS product ratio was calculated according to the law of propagation of error. Statistical difference in mdr1a/1b(-/-) mice were compared to normal mice by two-sided Student's *t* test with $p < 0.05$ as the limit of significance (* $p < 0.05$; ** $p < 0.01$).

the BBB, defined as the $K_{p, \text{brain}}$ ratio, correlated well with the function of *in vitro* P-gp, defined as the ratio of basal-to-apical flux to that of apical-to-basal flux in P-gp expressing LLC-PK1 divided by the same ratio in parental monolayer for 12 compounds ($r = 0.892$, $p < 0.01$) (20). Moreover, although the P-gp function in the BBB and the small intestine significantly correlated for the 12 compounds tested, the plot for

Table II. PS Products for the Transcellular Transport across MDR1 Expressing LLC-PK1 Monolayer

Drugs	$PS_{a \rightarrow b}$ ($\mu\text{L}/\text{min}/\text{mg}$ protein)		$PS_{a \rightarrow b}$ ratio
	LLC-MDR1	Parental	
Cimetidine	1.32 \pm 0.28	0.620 \pm 0.110	0.47 \pm 0.13
Cyclosporin A	0.98 \pm 0.07	1.59 \pm 0.12*	1.62 \pm 0.17
Daunomycin	2.64 \pm 0.27	1.75 \pm 0.04	0.66 \pm 0.07
Dexamethasone	1.89 \pm 0.19	1.85 \pm 0.05	0.98 \pm 0.10
Diazepam	3.78 \pm 0.03	3.94 \pm 0.26	1.04 \pm 0.07
Digoxin	0.560 \pm 0.058	1.03 \pm 0.21	1.84 \pm 0.42
Loperamide	11.3 \pm 0.1	16.4 \pm 0.4**	1.44 \pm 0.04
Progesterone	6.48 \pm 0.21	6.44 \pm 0.36	0.99 \pm 0.06
Quinidine	4.07 \pm 0.03	12.6 \pm 0.8**	3.09 \pm 0.19
Ritonavir	0.908 \pm 0.133	2.24 \pm 0.17**	2.47 \pm 0.41
Verapamil	7.51 \pm 0.14	12.5 \pm 0.1**	1.66 \pm 0.03
Vinblastine	1.39 \pm 0.01	1.56 \pm 0.09	1.12 \pm 0.07

Note: Based on the results shown in our previous report (20), the PS products for the transcellular transport (apical to basal) of 12 compounds were calculated. The values of *in vitro* PS product ratio ($PS_{a \rightarrow b}$ ratio), defined as the PS product for the apical-to-basal flux across the parental LLC-PK1 cells divided by the same value across MDR1-expressing LLC-PK1 monolayer, were also determined. The results are shown as the mean \pm SE. The SE of the $PS_{a \rightarrow b}$ ratio was calculated according to the law of propagation of error. Statistical difference in LLC-MDR1 cells were compared to parental cells by two-sided Student's *t* test with $p < 0.05$ as the limit of significance (* $p < 0.05$; ** $p < 0.01$).

$r = 0.855$
 $P < 0.01$

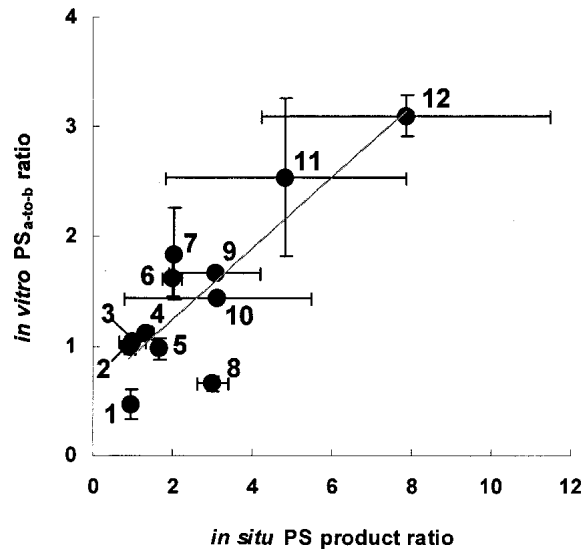


Fig. 4. Correlation of P-gp function determined in *in vitro* transcellular transport studies and in *in situ* intestinal perfusion studies. Data listed in Tables I and II were summarized to examine the correlation between *in situ* and *in vitro* P-gp function. Each point and vertical bar represents the mean \pm SE, which was calculated according to the law of propagation of error. Key: 1, cimetidine; 2, progesterone; 3, diazepam; 4, vinblastine; 5, dexamethasone; 6, cyclosporin A; 7, digoxin; 8, daunomycin; 9, verapamil; 10, loperamide; 11, ritonavir, 12, quinidine.

digoxin did not superimpose on the correlation line (Fig. 5). One of the reasons for the difference in the contribution of P-gp for digoxin between the BBB and the small intestine may be accounted for by the hypothesis that a transport

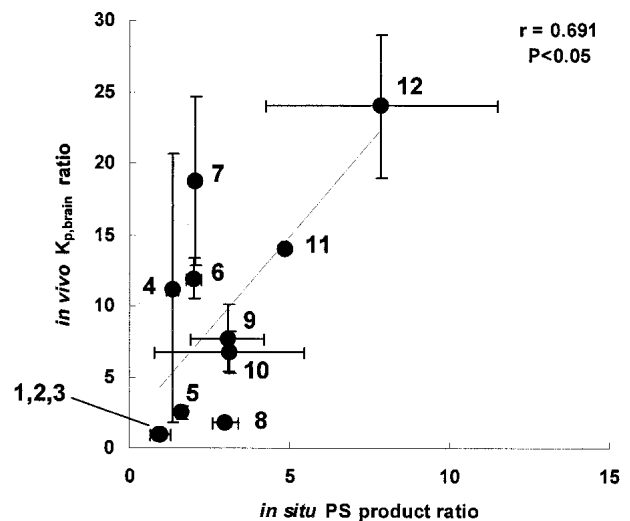
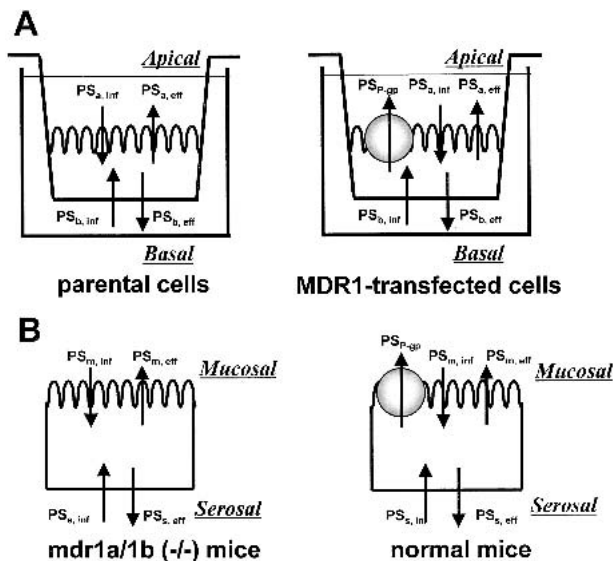


Fig. 5. Correlation of P-gp function determined in *in vivo* brain penetration studies and *in situ* intestinal perfusion studies. Data listed in Table I and those in our previous report (20) were summarized to examine the correlation of P-gp functions between the small intestine and the blood-brain barrier. Each point and vertical bar represents the mean \pm SE, which was calculated according to the law of propagation of error. Key: 1, cimetidine; 2, progesterone; 3, diazepam; 4, vinblastine; 5, dexamethasone; 6, cyclosporin A; 7, digoxin; 8, daunomycin; 9, verapamil; 10, loperamide; 11, ritonavir, 12, quinidine.



Scheme 1. Schematic diagram illustrating the PS products for the penetration of ligands across the cell monolayer. A and B represent the transcellular transport of ligands across the cultured cell monolayers and that across the intestinal epithelial cells, respectively. Key; $PS_{a,inf}$ and $PS_{a,eff}$ represent the PS products for the influx and efflux across the apical membrane, respectively. $PS_{b,inf}$ and $PS_{b,eff}$ represent the PS products for the influx and efflux across the basal membrane, respectively. PS_{P-gp} represents the PS product for P-gp-mediated efflux across the apical membrane. $PS_{m,inf}$ and $PS_{m,eff}$ represent the PS products for the influx and efflux across the mucosal membrane of intestinal epithelial cells, respectively. $PS_{s,inf}$ and $PS_{s,eff}$ represent the PS products for the influx and efflux across the serosal membrane of intestinal epithelial cells, respectively. PS_{P-gp} represents the PS product for the P-gp-mediated efflux across the mucosal membrane.

mechanism(s) other than P-gp is also involved in the intestinal absorption of digoxin. However, it may be not necessary for us to consider the involvement of *mdr1b* in the interpretation of the experimental data, since the predominant isoform in the BBB and the small intestine is *mdr1a* (25–27). In addition, it is also possible that the extent of intestinal metabolism is different between *mdr1a/1b* (-/-) and normal mice (28). Because we determined the total radioactivity in the outflow, it is plausible that the interpretation of the data may be subject to errors due to the presence of metabolites.

Finally, the fact that the absolute value of the slope (2.6) in Fig. 5 is significantly higher than one needs to be discussed. The difference in the contribution of P-gp in the BBB penetration determined by the $K_{p,brain}$ ratio and that in the intestinal absorption determined by the intestinal PS product ratio may be accounted for by considering the fact that the former is given by:

$$K_{p,brain} \text{ ratio} = 1 + \frac{PS_{P-gp}}{PS_{l,eff}} \quad (9)$$

where $PS_{l,eff}$ represents the PS product for the efflux across the luminal membrane. Obviously, Eqs. (5) and (9) differ from each other in that the denominator is $PS_{m,eff}$ plus $PS_{s,eff}$ in Eq. (5) whereas that in Eq. (9) is $PS_{l,eff}$, which accounts for the slope of 2.6 in Fig. 5. Alternatively, the results may also be due to a higher expression level of *mdr1a* in the BBB than in the small intestine.

In conclusion, we have quantified the contribution of P-gp to restricting the intestinal absorption of its substrate drugs. Such quantification is important in predicting the variation in the drug absorption due to interindividual differences in the expression level of intestinal P-gp and that due to simultaneously administered P-gp substrates/inhibitors. Moreover, we have also found that the *in vitro* transcellular transport across P-gp expressing monolayers may be used to predict the intestinal P-gp function, although the correlation coefficient was lower than that observed between the P-gp function in the BBB and *in vitro* model.

ACKNOWLEDGMENTS

This work was supported by Grant-in-Aid for Scientific Research on Priority Areas ABC proteins 10044243 and on Priority Areas epithelial vectorial transport 12144201 from the Ministry of Education, Science and Culture of Japan.

REFERENCES

- C. J. Chen, J. E. Chin, K. Ueda, D. P. Clark, I. Pastan, M. M. Gottesman, and I. B. Roninson. Internal duplication and homology with bacterial transport proteins in the *mdr1* (P-glycoprotein) gene from multidrug-resistant human cells. *Cell* **47**:381–389 (1986).
- K. Ueda, D. P. Clark, C. J. Chen, I. B. Roninson, M. M. Gottesman, and I. Pastan. The human multidrug resistance (*mdr1*) gene. cDNA cloning and transcription. *J. Biol. Chem.* **262**:505–508 (1987).
- S. V. Ambudkar, S. Dey, C. A. Hrycyna, M. Ramachandra, I. Pastan, and M. M. Gottesman. Biochemical, cellular, and pharmacological aspects of the multidrug transporter. *Annu. Rev. Pharmacol. Toxicol.* **39**:361–398 (1999).
- V. J. Wacher, J. A. Silverman, Y. Zhang, and L. Z. Benet. Role of P-glycoprotein and cytochrome P450 3A in limiting oral absorption of peptides and peptidomimetics. *J. Pharm. Sci.* **87**:1322–1330 (1998).
- L. Z. Benet, T. Izumi, Y. Zhang, J. A. Silverman, and V. J. Wacher. Intestinal MDR transport proteins and P450 enzymes as barriers to oral drug delivery. *J. Control. Release* **62**:25–31 (1999).
- A. H. Schinkel. Pharmacological insights from P-glycoprotein knockout mice. *Clin. Pharmacol. Ther.* **36**:9–13 (1998).
- A. Sparreboom, J. van Asperen, U. Mayer, A. H. Schinkel, J. W. Smit, D. K. F. Meijer, P. Borst, W. J. Nooijen, J. H. Beijnen, and O. van Tellingen. Limited oral bioavailability and active epithelial excretion of paclitaxel (Taxol) caused by P-glycoprotein in the intestine. *Proc. Natl. Acad. Sci. USA* **94**:2031–2035 (1997).
- H. A. Bardelmeijer, J. H. Beijnen, K. R. Brouwer, H. Rosing, W. J. Nooijen, J. H. M. Schellens, and O. van Tellingen. Increased oral bioavailability of paclitaxel by GF120918 in mice through selective modulation of P-glycoprotein. *Clin. Cancer Res.* **6**:4416–4421 (2000).
- U. Mayer, E. Wagenaar, J. H. Beijnen, J. W. Smit, D. K. F. Meijer, J. van Asperen, P. Borst, and A. H. Schinkel. Substantial excretion of digoxin via the intestinal mucosa and prevention of long term of digoxin accumulation in the brain by the *mdr1a* P-glycoprotein. *Br. J. Pharmacol.* **129**:1038–1044 (1996).
- K. Yokogawa, M. Takahashi, I. Tamai, H. Konishi, M. Nomura, S. Moritani, K. Miyamoto, and A. Tsuji. P-glycoprotein-dependent disposition kinetics of tacrolimus: studies in *mdr1a* knockout mice. *Pharm. Res.* **16**:1213–1218 (1999).
- R. B. Kim, M. F. Fromm, C. Wandel, B. Leake, A. J. J. Wood, D. M. Roden, and G. R. Wilkinson. The drug transporter P-glycoprotein limits oral absorption and brain entry of HIV-1 protease inhibitors. *J. Clin. Invest.* **101**:289–294 (1998).
- C. B. Washington, H. R. Wiltshire, M. Man, T. Moy, S. R. Harris, E. Worth, P. Weigl, Z. Liang, D. Hall, L. Marriotti, and T. F. Blaschke. The disposition of saquinavir in normal and p-glycoprotein deficient mice, rats, and in cultured cells. *Drug Metab. Dispos.* **28**:1058–1062 (2000).

13. B. Greiner, M. Eichelbaum, P. Fritz, H. P. Kreichgauer, O. von Richter, J. Zundler, and H. K. Kroemer. The role of intestinal P-glycoprotein in the interaction and rifampin. *J. Clin. Invest.* **104**:147–153 (1999).
14. K. S. Lown, R. R. Mayo, A. B. Leichtman, H. L. Hsiao, K. Turgeon, P. Schmielkin-Ren, M. B. Brown, W. Guo, S. J. Rossi, L. Z. Benet, and P. B. Watkins. Role of intestinal P-glycoprotein (*mdr1*) in interpatient variation in the oral bioavailability of cyclosporine. *Clin. Pharmacol. Ther.* **62**:248–260 (1997).
15. D. J. Edwards, M. E. Fitzsimmons, E. G. Schuetz, K. Yasuda, M. P. Ducharme, L. H. Warbasse, P. M. Moster, J. D. Schuetz, and P. Watkins. 6',7'-Dihydroxybergamottin in grapefruit juice and Seville orange juice: Effect on cyclosporin disposition, enterocyte CYP3A4, and P-glycoprotein. *Clin. Pharmacol. Ther.* **65**:237–244 (1999).
16. N. von Ahsen, M. Richter, C. Grupp, B. Ringe, M. Oellerich, and V. W. Armstrong. No influence of the MDR-1 C3435T polymorphism or a CYP3A4 promoter polymorphism (CYP3A4-V Allele) on dose-adjusted cyclosporin A trough concentration or rejection incidence in stable renal transplant recipients. *Clin. Chem.* **47**:1048–1052 (2001).
17. S. Hoffmeyer, O. Burk, O. von Richter, H. P. Arnold, J. Brockmüller, A. Johné, I. Cascorbi, T. Gerloff, I. Roots, M. Eichelbaum, and U. Brinkmann. Functional polymorphisms of the human multidrug-resistance gene: Multiple sequence variations and correlation of one allele with P-glycoprotein expression and activity *in vivo*. *Proc. Natl. Acad. Sci. USA* **97**:3473–3478 (2000).
18. R. B. Kim, B. F. Leake, E. F. Choo, G. K. Dresser, S. V. Kubba, U. I. Schwarz, A. Taylor, H. G. Xie, J. McKinsey, S. Zhou, L. B. Lan, J. D. Schuetz, E. G. Schuetz, and G. R. Wilkinson. Identification of functional variant MDR1 alleles among European Americans and African Americans *Clin. Pharmacol. Ther.* **70**: 189–199 (2001).
19. J. Fellay, C. Marzolini, E. R. Meaden, D. J. Back, T. Buclin, J. Chave, L. A. Decosterd, H. Furrer, M. Opravil, G. Pantaleo, D. Retelska, L. Ruiz, A. H. Schinkel, P. Vernazza, C. B. Eap, and A. Telenti. Response to antiretroviral treatment in HIV-1-infected individuals with the allelic variants of the multidrug resistance transporter 1: a pharmacogenetics study. *Lancet* **359**:30–36 (2002).
20. Y. Adachi, H. Suzuki, and Y. Sugiyama. Comparative studies on *in vitro* methods for evaluating *in vivo* function of MDR1 P-glycoprotein. *Pharm. Res.* **18**:1660–1668 (2001).
21. M. Yamazaki, W. E. Neway, T. Ohe, I. Chen, J. F. Rowe, J. H. Hochman, M. Chiba, and J. H. Lin. *In vitro* substrate identification studies for P-glycoprotein-mediated transport: species difference and predictability of *in vivo* results. *J. Pharmacol. Exp. Ther.* **296**:723–735 (2001).
22. R. M. Loria, H. L. Kayne, S. Kibrick, and S. A. Broitman. Measurement of intestinal absorption in mice by a double-label radioisotope perfusion technic. *Lab. Animal Sci.* **26**:603–606 (1976).
23. H. Yuasa and K. Matsuda. and J. Watanabe. Influence of anesthetic regimens on intestinal absorption in rats. *Pharm. Res.* **10**: 884–888 (1993).
24. L. Barthe, J. Woodley, and G. Houin. Gastrointestinal absorption of drugs: methods and studies. *Fundam. Clin. Pharmacol.* **13**:154–168 (1999).
25. A. H. Schinkel, C. A. A. M. Mol, E. Wagenaar, L. van Deemter, J. J. M. Smit, and P. Borst. Multidrug resistance and the role of P-glycoprotein knockout mice. *Eur. J. Cancer* **31A**:1295–1298 (1995).
26. P. Borst, A. H. Schinkel, J. J. M. Smit, E. Wagenaar, L. van Deemter, A. J. Smith, E. W. H. M. Eijdem, F. Baas, and G. J. R. Zaman. Classical and novel forms of multidrug resistance and the physiological function of P-glycoproteins in mammals. *Pharmacol. Ther.* **60**:289–299 (1994).
27. Y. Zhang and L. Z. Benet. The gut as a barrier to drug absorption. *Clin. Pharmacokinet.* **40**:159–168 (2001).
28. E. G. Schuetz, D. R. Unbenhauer, K. Yasuda, C. Brimer, L. Nguyen, M. V. Relling, J. D. Schuetz, and A. H. Schinkel. Altered expression of hepatic cytochromes P-450 in mice deficient in one or more *mdr1* genes. *Mol. Pharmacol.* **57**:188–197 (2000).